# Si incorporation and Burstein–Moss shift in *n*-type GaAs

M.K. Hudait [a,b], P. Modak [b], S.B. Krupanidhi [a,*]

[a] *Materials Research Centre, Indian Institute of Science, Bangalore-560 012, India*
[b] *Central Research Laboratory, Bharat Electronics, Bangalore-560 013, India*

## Abstract

Silane ($SiH_4$) was used as an *n*-type dopant in GaAs grown by low pressure metalorganic vapor phase epitaxy using trimethylgallium (TMGa) and arsine ($AsH_3$) as source materials. The electron carrier concentrations and silicon (Si) incorporation efficiency are studied by using Hall effect, electrochemical capacitance voltage profiler and low temperature photoluminescence (LTPL) spectroscopy. The influence of growth parameters, such as $SiH_4$ mole fraction, growth temperature, TMGa and $AsH_3$ mole fractions on the Si incorporation efficiency have been studied. The electron concentration increases with increasing $SiH_4$ mole fraction, growth temperature, and decreases with increasing TMGa and $AsH_3$ mole fractions. The decrease in electron concentration with increasing TMGa can be explained by vacancy control model. The PL experiments were carried out as a function of electron concentration ($10^{17} - 1.5 \times 10^{18}$ cm$^{-3}$). The PL main peak shifts to higher energy and the full width at half maximum (FWHM) increases with increasing electron concentrations. We have obtained an empirical relation for FWHM of PL, $\Delta E(n)$ (eV) $= 1.4 \times 10^{-8} n^{1/3}$. We also obtained an empirical relation for the band gap shrinkage, $\Delta E_g$ in Si-doped GaAs as a function of electron concentration. The value of $\Delta E_g$ (eV) $= -2.75 \times 10^{-8} n^{1/3}$, indicates a significant band gap shrinkage at high doping levels. These relations are considered to provide a useful tool to determine the electron concentration in Si-doped GaAs by low temperature PL measurement. The electron concentration decreases with increasing TMGa and $AsH_3$ mole fractions and the main peak shifts to the lower energy side. The peak shifts towards the lower energy side with increasing TMGa variation can also be explained by vacancy control model. © 1999 Elsevier Science S.A. All rights reserved.

*Keywords:* Gallium arsenide; Optical properties; Photoluminescence; Semiconductors

## 1. Introduction

Metalorganic vapor phase epitaxy (MOVPE) [1] is one of the premier techniques for the fabrication of GaAs-based structures for optoelectronic device applications. Improvements in processing technology are needed to optimize film composition, thickness and doping uniformity over large areas in order to maximize the yield and throughput. This is primarily important for optoelectronic devices, where device characteristics are strongly dependent on the physical and electrical properties of epitaxial layers. In this case, only a few percent spread in the film thickness and dopant concentration can be tolerated for uniform device performance [2]. This level of control over film properties can only be achieved through a detailed understanding of the fundamental processes underlying the film growth and dopant incorporation in MOVPE. Therefore, it is necessary to understand the influence of the growth parameters, which control accurate doping and nature of interfaces for good characteristics of the devices.

The effect of *n*-type heavy doping in GaAs is an important issue of the optical and electrical properties not only from a fundamental understanding but also for the device applications, such as contact layer of double heterojunction bipolar transistor (DHBTs), laser diodes, solar cells, metal semiconductor field effect transistors (MESFETs) and high electron mobility transistors (HEMTs). The heavy doping affects the density of states, band structure, carrier mobility, absorption, luminescence properties and hence the device properties. For example, the heavy doping is used either in the source and drain of MESFETs or active layer of laser diode. Also, the heavy doping produces some changes in band structure of semiconductors. One of the

* Corresponding author. Tel.: +91-80-3311330; Fax: +91-80-3341683.

*E-mail address:* sbk@mrc.iisc.ernet.in (S.B. Krupanidhi)

changes is band gap narrowing (BGN) or band gap shrinkage due to the formation of density-of-states, and the tails are resulted from inhomogeneous impurity distribution [3]. The inhomogeneous impurity distributions also imply the fluctuations in potential which destroy the translational symmetry of the crystal and it allows the $k$-nonconserving transitions, i.e. the indirect transitions. Another important phenomenon occurring in the heavily donor-doped semiconductors is an increase in the interband transition energy due to the filling of the conduction band by electrons, which is known as the Burstein–Moss effect [4]. Band gap shrinkage due to heavy doping is a well known phenomenon in III-V compound semiconductors, particularly observed in GaAs by photoluminescence (PL) spectroscopy [3,5–11]. In the heterojunction-based devices, the band gap shift due to heavy doping result in valence and conduction band discontinuity of the heterojunction interface [12]. Both the band gap narrowing and Fermi energy, $\varepsilon_f$, of heavily doped GaAs were analyzed as a function of doping concentration $n$ using PL [3,5–11] and cathdoluminescence [13]. The reported band gap narrowing was either proportional to $n^{1/3}$ [3,5] or $n^{5/12}$ [6,13]. Some low temperature PL (LTPL) results were explained by assuming that the Fermi energy relative to the conduction band minimum depends on $n$ by the $n^{2/3}$ power rule for $n \geq 10^{18}$ cm$^{-3}$ [6]. In the LTPL experiments, the donor–acceptor (D–A) pair luminescence is dominant for electron concentrations less than $1 \times 10^{18}$ cm$^{-3}$, while the indirect (without $k$-selection) band to band (B–B) or band to acceptor (B–A) transitions prevail at higher concentrations [6,8]. The emission spectrum of a heavily doped semiconductor consists of a single and broad structure usually attributed to B–B recombination. The low energy side of the band is related to the BGN and to the tailing of the density-of-states; the higher energy side of the spectrum reveals band filling by the majority carriers and provides information about the $\varepsilon_f$ position [14].

The $n$-type doping in GaAs can be obtained by using Si [15,16], S [17,18], Ge [19], Sn [20], Se [21], or Te [22] as doping sources. Among these doping sources Si is commonly used as an intentional $n$-type dopant in GaAs and related compounds. It has an extremely low diffusivity in GaAs [23], which makes it attractive for device fabrications involving high temperature post-growth processing steps. In III–V semiconductors, Si a group IV element can act as either an acceptor or donor, depending on the sublattice where it populates. In MOVPE grown GaAs and AlGaAs, Si has been found almost exclusively to occupy group III sites and function as a donor. The site selection of Si depends on the thermodynamic growth conditions [15]. In As-rich MOVPE growth, Si incorporates exclusively on Ga sites up to a concentration of $\sim 5 \times 10^{18}$ cm$^{-3}$ [24] at which point it also begins to occupy arsenic sites, acting

as an acceptor. This solubility limitation results in self-compensation and limits the maximum carrier concentration that can be obtained with Si [24]. The generation of Ga vacancy ($V_{Ga}$), which is negatively charged at higher concentration compensates the carrier in $n^+$-type GaAs [25,26].

The most commonly used Si dopant sources are silane (SiH$_4$) and disilane (Si$_2$H$_6$). Because of the differences in electrical and optical properties of Si-doped GaAs from S, Te, Sn, Ge, Se-doped GaAs grown by metalorganic vapor phase epitaxy (MOVPE), these properties were studied extensively by several authors in recent years [17–22]. However, significant variation of the growth parameters was needed to obtain the incorporation of controlled amount of impurities in MOVPE growth process. Since, Si has extremely low diffusivity in GaAs, it prompted us to conduct a systematic study of Si doping in GaAs by MOVPE approach.

PL spectroscopy is the most common characterization technique for investigating the distribution of defects, concerning the type and heavy doping effect in GaAs, hence employed in our work. It is a nondestructive and noncontact technique for examining the band structure and luminescence properties of GaAs. The luminescence properties are dependent on the growth conditions (or methods), impurity species, doping concentrations and growth temperatures. PL spectroscopy has also been employed to investigate the Fermi level of heavily $n$-type doped materials [6,10], the carrier concentration [27] and the epitaxial layer quality [28]. The effect of growth parameters, such as SiH$_4$ mole fraction, growth temperature, arsine (AsH$_3$) and trimethylgallium (TMGa) mole fractions on Si incorporation in GaAs are investigated thoroughly and these results are compared with the published literatures [5,29–31]. After thorough investigation of Si-doped GaAs, we have suggested a relationship of full width at half maximum (FWHM) and band gap shrinkage versus electron concentration of Si-doped GaAs, which could be considered a useful tool to determine the electron concentration in Si-doped GaAs by low temperature PL measurement. The electron concentration increases with increasing SiH$_4$ mole fraction, growth temperature and decreases with AsH$_3$ and TMGa mole fractions. A vacancy control model was found to be suitable to explain our results with TMGa variation.

## 2. Experimental details

The Si-doped $n$-type GaAs were grown in a low pressure horizontal MOVPE reactor on both Cr-doped semi-insulating and Si-doped $n^+$-GaAs (100) substrates with an offset by 2° towards (110) direction. The source materials were trimethylgallium (TMGa), (100%) arsine (AsH$_3$), (104 ppm) silane (SiH$_4$) as an $n$-type dopant

and palladium purified $H_2$ as a carrier gas. During the growth, the pressure inside the reactor was kept at 100 Torr and the growth temperature was varied from 600 to 725°C. TMGa and $AsH_3$ flow rate was varied from 10 to 20 SCCM and 30 to 50 SCCM, respectively. The total flow rate was about 2 SLPM.

The doping concentrations were determined by using both Bio-Rad electrochemical capacitance voltage (ECV) polaron profiler and Hall measurement. Hall effect measurements (Van der Pauw method) were carried out at 300 K to determine the mobility (Hall factor $r_H = 1$). N-Type layers with thickness of about 2 μm were chosen for analysis to reduce thickness measurement errors. Electron densities in the range of $10^{17} - 1.5 \times 10^{18}$ cm$^{-3}$ were measured.

PL measurements were carried out using a MIDAC Fourier Transform PL (FTPL) system at a temperature of 4.2 K and 100 mW laser power. An argon ion laser operating at a wavelength of 5145 Å was used as a source of excitation. The exposed area was about 3 mm$^2$. PL signal was detected by a LN$_2$ cooled Ge-Photodetector whose operating range is about 0.75–1.9 eV, while resolution was kept at about 0.5 meV.

## 3. Results and discussion

### 3.1. Electrical properties

#### 3.1.1. Effect of variation of SiH$_4$ mole fraction and growth temperature

The surface of epilayers is influenced by the growth parameters, such as pressure inside the reactor tube, growth temperature, substrate orientation, AsH$_3$/TMGa (so called V/III ratio) mole ratio, etc. The surface of Si-doped $n$-type GaAs appears to be mirror smooth over a wide range of temperatures (600–725°C) in this study. Fig. 1 shows the electron concentration as a function of SiH$_4$ mole fraction.

The electron concentration increases monotonically with SiH$_4$ mole fraction, which is consistent to that described by Bass [19] and compensates at the concentration of $n > 1.5 \times 10^{18}$ cm$^{-3}$. Since Si is a low vapor pressure element ($10^{-11}$ Torr at 600°C), the concentration of Si incorporated in GaAs during MOVPE growth depends on the ratio of the inlet mole fraction of SiH$_4$ to the inlet mole fraction of TMGa, $[Si]_{GaAs} \propto (x_{dopant}/x_{TMGa})$. This ratio is commonly reported in experimental studies of Si doping. Si doping, therefore, increases linearly with an increase in the inlet dopant mole fraction and is inversely proportional to the growth rate of GaAs. In MOVPE growth, Si the amphoteric dopant is found to incorporate preferentially on one sublattice over a fairly wide range of dopant concentrations. At high dopant concentrations, however, population of the other sublattice can become

energetically more favourable resulting in both donor and acceptor formation. This autocompensation limits the maximum carrier concentration that can be achieved in the semiconductor with an amphoteric dopant. The incorporation of an amphoteric dopant on a particular site is considered to result from the combination of thermodynamic, electronic and chemical effects [32]. The electron concentration increases with increasing SiH$_4$ up to $2.9 \times 10^{-5}$ Torr and then decreases due to autocompensation. The autocompensation can be confirmed by considering the optical properties of the films using low temperature PL spectroscopy as an experimental tool. This has been discussed in Section 3.2.1 on the optical properties of the films by PL spectroscopy. We are assuming that the amount of Si concentration and electron concentration are the same up to a Si doping concentration of $1.5 \times 10^{18}$ cm$^{-3}$ in our present growth conditions and this is consistent with that reported in the literature [33]. However, as the doping concentration increased further, the inactivated concentration increased relatively with the doped concentration, indicating the limits of free carrier concentration. The decrease of free-carrier concentration in heavily doped $n$-type GaAs is a well-known phenomenon based upon two main models. One involves amphoteric native defects with strong Fermi level dependent defect formation energy [25,26] and the other involves electronic occupation of a highly localized state of the donor-related DX center [34]. In the recent study of Si-doped GaAs by Fushimi et al. [33], they pointed out that the limit of free-carrier concentration
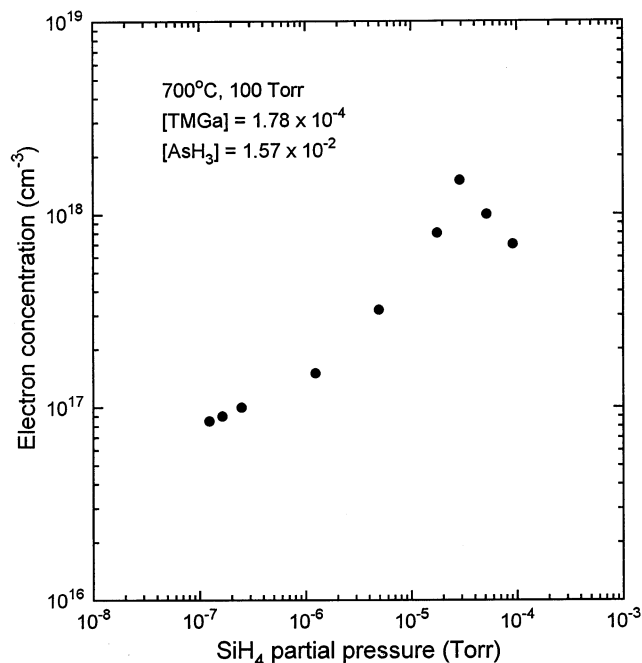


Fig. 1. Electron concentration of Si-doped GaAs as a function of SiH$_4$ partial pressure.

in the heavily doped layers is caused by gallium vacancy ($V_{Ga}$) and not by electron occupation of a highly localized state of the donor-related DX center.

It is well accepted that at low Si concentrations, the Si atoms enter into the lattice mainly as a simple substitutional impurity at the group III element sites (Ga), acting as a donor ($Si_{Ga}$) and at the As sites, acting as an acceptor ($Si_{As}$) [35–38]. The latter become increasingly important as the Si concentration increases, causing a saturation of the free electron concentration. Heavily doped films present a strong compensation of the free electron concentration. This compensation has been attributed in GaAs mainly to a complex defect formed by a donor atom coupled to a group III element vacancy ($Si_{Ga}-V_{Ga}$), the so-called self-activating center [39]. This complex defect gives rise to a broad photoluminescence line centered about 1.2 eV for GaAs [40] and 1.35 eV for $Al_{0.3}Ga_{0.7}As$ [39] samples. Another deep photoluminescence feature about 1.05–1.28 eV has been attributed to a $Si_{Ga}-Si_{As}$ pair defect [41,42], and responsible for the compensation. Maguire et al. [43] investigated Si doped GaAs by using local vibration modes (LVM), Hall effect, and secondary ion mass spectroscopy (SIMS) and concluded that the [Si–X] was tentatively attributed to the well-known self-activated center ($Si_{Ga}-V_{Ga}$). The LVM results do not necessarily exhaust the possibilities of forms of Si incorporation. Souza and Rao [41] mentioned that in GaAs, the Si incorporation is extremely complex and highly dependent on growth conditions. We showed some evidence of the presence of $Si_{Ga}-Si_{As}$ pair defects by studying samples grown under different $SiH_4$ partial pressures and different growth temperatures. These $Si_{Ga}-Si_{Ag}$ defect pairs are responsible for reducing free-carrier concentration of higher Si doping levels due to compensation effects. The detailed discussion regarding the autocompensation can be found in Section 3.2.1.

The electron concentration is observed to increase as the growth temperature increases as shown in Fig. 2 for a fixed $SiH_4$ mole fraction, with an apparent activation energy for doping of 1.47 eV [44]. The strong temperature dependence of Si incorporation is believed to be a result of increasing decomposition rate of $SiH_4$ with increasing temperature. The activation energy for doping ($E_a$) can be defined as:

$$n \propto P^0_{SiH_4} \exp(-E_a/KT) \qquad (1)$$

where $n$ is the measured electron concentration and $P^0_{SiH4}$ is the inlet partial pressure of $SiH_4$. The electron concentration is equivalent to the Si concentration in most cases ($n \approx [Si]_{GaAs}$). For a given TMGa, $SiH_4$ and $AsH_3$ mole fractions, the electron concentration and Hall mobility are also shown in Fig. 2. The electron mobility exhibits a decrease with increasing growth temperature. From this figure, it is also seen that the electron concentration decreases with increasing growth
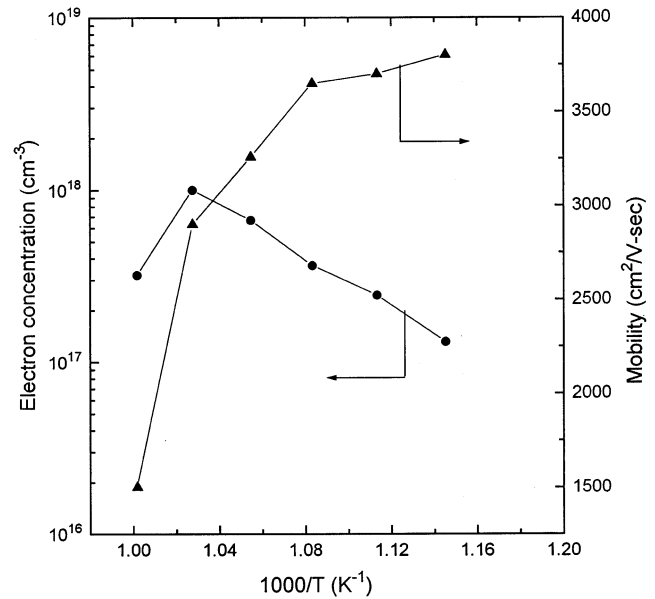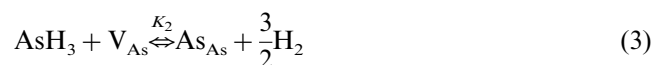


Fig. 2. A 300 K electron carrier concentrations and electron mobilities for Si-doped GaAs epilayers grown under various growth temperatures. The growth parameters are: $[SiH_4] = 5.18 \times 10^{-7}$, $[TMGa] = 1.78 \times 10^{-4}$ and $[AsH_3] = 1.57 \times 10^{-2}$.

temperature above 700°C due to autocompensation and is further confirmed by the Hall mobility data. The autocompensation was further confirmed by the LTPL results presented in Section 3.2.2 on the optical properties of Si-doped GaAs.

### 3.1.2. Effect of TMGa mole fraction

The electron concentration versus TMGa mole fraction is illustrated in Fig. 3, for a given $AsH_3$ and $SiH_4$ mole fraction. The electron concentration decreases with increasing TMGa flow rates, which is in agreement with the earlier reported results by Field and Ghandhi [16] and Duchemin et al. [45]. A vacancy-controlled model may be considered to explain such behavior. In the $TMGa-AsH_3$ system, the leading reaction to the formation of GaAs can be expressed as:

$$(CH_3)_3Ga + \frac{3}{2}H_2 + V_{Ga} \overset{K_1}{\Leftrightarrow} Ga_{Ga} + 3CH_4 \qquad (2)$$

$$AsH_3 + V_{As} \overset{K_2}{\Leftrightarrow} As_{As} + \frac{3}{2}H_2 \qquad (3)$$

Where $K_1$ and $K_2$ are the equilibrium constants of the above reactions, then

$$\frac{[V_{Ga}]}{[V_{As}]} \equiv \frac{K_2}{K_1} \frac{P^3_{CH_4}}{P_{TMGa}} \frac{P_{AsH_3}}{P^3_{H_2}} \qquad (4)$$

Since Si as a donor is on the Ga sublattice and under equilibrium, its incorporation should be proportional to the concentration of Ga vacancies, $[V_{Ga}]$ [19]. The doping reaction is:

$$SiH_4 + V_{Ga} \overset{K_3}{\to} Si_{Ga} + 2H_2 \qquad (5)$$

From Eqs. (4) and (5) one can write,

$$\frac{[Si_{Ga}]}{[V_{As}]} \equiv \frac{K_2 K_3}{K_1} \frac{P_{SiH_4}}{P_{TMGa}} \frac{P_{AsH_3}}{P_{H_2}^5} P_{CH_4}^3 \qquad (6)$$

A decrease in $P_{TMGa}$ will increase in gallium vacancy concentration, hence, the incorporation of Si on Ga site is increased. The electron concentration is thus increased when the TMGa mole fraction is decreased.

### 3.1.3. Effect of AsH₃ mole fraction

We also studied the electrical and optical properties of low-doped layers grown with increasing $AsH_3$ mole fraction to check if there is an amphoteric effect of Si. The electron concentration versus $AsH_3$ mole fraction is illustrated in Fig. 4, for a given TMGa and $SiH_4$ mole fractions. The electron concentration decreases very slowly with increasing $AsH_3$ flow rates. According to the above model, as the $AsH_3$ partial pressure is increased, the $[V_{Ga}]$ concentration increases and therefore the Si donor level should also increase. Conversely, as the $AsH_3$ partial pressure decreases, the As vacancies should increase and the Si as an acceptor should increase. The fact that the reverse behavior takes place suggests that the incorporation of Si is not controlled by the bulk thermodynamic properties of the lattice but by the surface kinetic process; the As appears to block the Si from the growing surface [19]. But we found that for a fixed concentration of $SiH_4$ mole fraction, the electron concentration decreases with increasing $AsH_3$
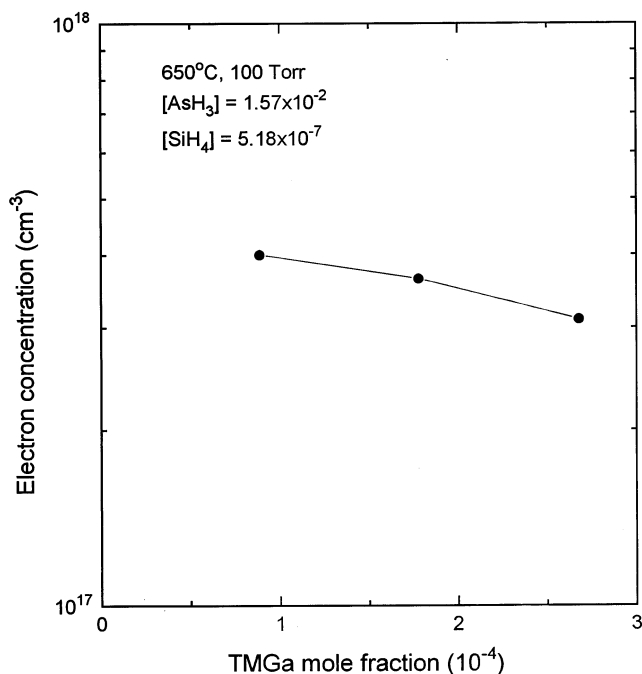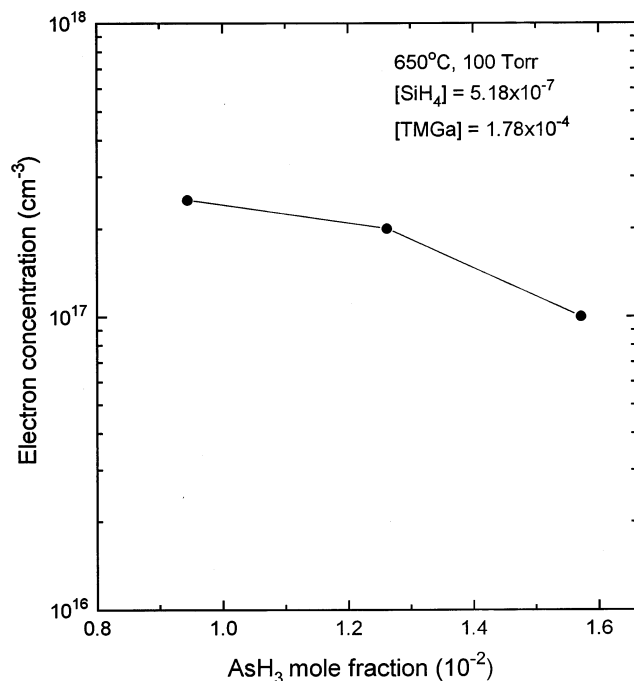
Fig. 4. Electron concentration as a function of AsH₃ mole fraction.

concentration, which is in agreement with the results reported by Field and Ghandhi [16] and Bass [19].

### 3.2. Optical properties

#### 3.2.1. PL spectra as a function of electron concentration

Fig. 5 shows the 4.2 K PL spectra of Si-doped GaAs for electron concentrations of (a) $1 \times 10^{17}$ cm⁻³; (b) $1.5 \times 10^{17}$ cm⁻³; (c) $3.2 \times 10^{17}$ cm⁻³; (d) $8 \times 10^{17}$ cm⁻³; (e) $9 \times 10^{17}$ cm⁻³; (f) $1.5 \times 10^{18}$ cm⁻³; (g) $1 \times 10^{18}$ cm⁻³; and (h) $7 \times 10^{17}$ cm⁻³, respectively. The curves were intentionally offset along $y$-axis with respect to each other for better clarity. The same procedure was used for all other PL spectra in this paper. When the electron concentration is relatively low, the PL spectra is symmetric and at higher concentrations becomes asymmetric. This tendency of slopes in the low-energy and high-energy side of the PL spectra is compared with those of the low-temperature PL spectra of heavily-doped $n$-type GaAs [5,6,8]. But Lee et al. [10] found the asymmetric nature of the PL peak at lower concentration of Si-doped GaAs grown by molecular beam epitaxy (MBE). The Si doping broadens the excitonic emission until it becomes a wide band-to-band luminescence. The peak at 1.493 eV has been attributed to band to acceptor (B–A) transitions involving residual carbon (C) impurities present in MOVPE GaAs [46]. The energy separation between the B–A peak and the B–B peak (band gap of GaAs at 4.2 K is 1.5194 eV) is consistent with typical acceptor ionization ener-

Fig. 3. Electron concentration as a function of TMGa mole fraction.

gies such as that of C ($E_a \sim 26.4$ meV) [47], which is a p-type dopant in MOVPE. This B–A transition is observed at electron concentration of $1 \times 10^{17}$ cm$^{-3}$ and the peak height decreases with increasing doping concentration. The similar type of observation was made by Sieg and Ringel [48] in MOVPE grown Si-doped InP by 16 K PL measurement. De-Sheng et al. [6] found that for electron concentrations below $5 \times 10^{17}$ cm$^{-3}$ of Te doped GaAs grown by MBE, B–A transitions involving residual C acceptors act as dominant recombination process. Above $10^{18}$ cm$^{-3}$, however, the luminescence spectra can be well described by indirect transitions between free electrons in the conduction band and localized acceptor—like centers in the deeper tail states above the valence band edge. Beyond $3.2 \times 10^{17}$ cm$^{-3}$ in our case, only one broad emission band is found, and the peak maximum of the dominant emission $E_{max}$ is shifted monotonically towards higher energy with increasing free-carrier concentration. According to Burstein and Moss [4], this shift results from the filling of the conduction band. The Burstein–Moss shift is more pronounced in n-type GaAs than p-type material because of the lower density of states at the bottom of the conduction band. When
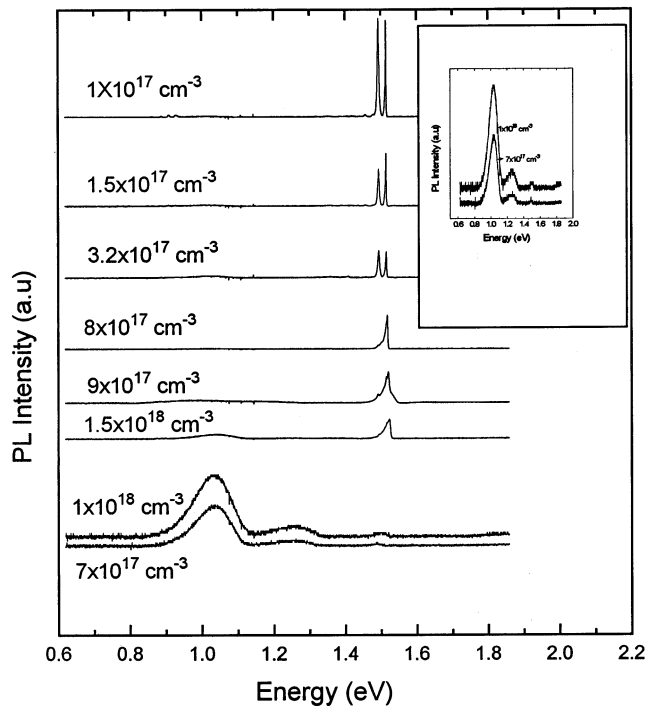
the free-carrier concentration in the sample exceeding $3.2 \times 10^{17}$ cm$^{-3}$, the spectral shape of the main emission peak becomes strongly asymmetric having a steep slope on the high-energy side and a smooth slope on the low-energy side of the spectra. The maxima of the luminescence peaks always show up on the high-energy side of the bands. The symmetry of the PL spectra was obtained by temperature variations of asymmetric PL spectra at higher concentration [6]. The asymmetry observed in the spectra of Fig. 5 at $n > 3.2 \times 10^{17}$ cm$^{-3}$ strongly indicates that indirect (without k-selection) B–B or B–A transitions dominate the emission across the optical gap. The contribution of indirect transitions in the luminescence of degenerate n-type semiconductors has recently been reported for n-type InP [48] and n-InAs [49]. With increasing electron concentration, however, the development of a density-of-states tail in the energy gap due to inhomogeneous impurity distribution and potential fluctuations in heavily doped semiconductors becomes more important for the radiative recombination process. The localized states in such a band tail can be treated as acceptor-like centers distributed above the top of the valence band as proposed by Levanyuk and Osipov [50].

From Fig. 5, it is seen that the sample is autocompensated, when the electron concentration is greater than $1.5 \times 10^{18}$ cm$^{-3}$ in our present growth conditions. The PL spectra corresponding to the electron concentrations $1 \times 10^{18}$ and $7 \times 10^{17}$ cm$^{-3}$ are plotted inset in Fig. 5. In addition to the near band peak, one observes a broad band with different peaks at around 1.05 and 1.2558 eV. The presence of these peaks leads one to believe that possibly this PL band involves more than one emission. In these PL spectra, one can find that as Si partial pressure increases the lower energy emissions are more favoured. These deep photoluminescence feature at about 1.05–1.28 eV has been attributed to a $Si_{Ga}$–$Si_{As}$ pair defect [41,42]. The 1.20 eV PL emission in GaAs has been extensively studied and is attributed to the complex ($Si_{Ga}$–$V_{Ga}$) [51]. A peak at around 1.4894 eV was observed at higher doping level, most clearly seen at the $SiH_4$ partial pressure greater than $2.9 \times 10^{-5}$ Torr of inset Fig. 5. The peak is probably associated with the shallow acceptor, $Si_{As}$ [51]. The broad, lower energy emission with a peak energy of $\approx 1.05$ eV (inset Fig. 5) is accompanied with the $Si_{Ga}$–$V_{Ga}$ complex for the highest $SiH_4$ partial pressure. During the process of identifying this characteristics emission it should be kept in mind that the Si concentration is high and that even Si precipitates have been formed [52]. Therefore, $Si_{Ga}$ atoms remain present in the solid, and their concentration may even have increased at this higher $SiH_4$ concentrations. Gallium vacancies, however, could have been occupied by additional Si atoms. Hence, the simplest mode of understanding is to replace the gallium vacancy in the



Fig. 5. A 4.2 K PL spectra of Si-doped GaAs epilayers for various electron concentrations. The electron concentrations are: (a) $1 \times 10^{17}$ cm$^{-3}$; (b) $1.5 \times 10^{17}$ cm$^{-3}$; (c) $3.2 \times 10^{17}$ cm$^{-3}$; (d) $8 \times 10^{17}$ cm$^{-3}$; (e) $9 \times 10^{17}$ cm$^{-3}$; (f) $1.5 \times 10^{18}$ cm$^{-3}$; (g) $1 \times 10^{18}$ cm$^{-3}$; and (h) $7 \times 10^{17}$ cm$^{-3}$. The inset shows the electron concentrations due to $1 \times 10^{18}$ and $7 \times 10^{17}$ cm$^{-3}$, respectively. The growth parameters are: Substrate temperature, 700°C, [TMGa] $= 1.78 \times 10^{-4}$, [AsH$_3$] $= 1.57 \times 10^{-2}$ and SiH$_4$ partial pressure ranging from $1.24 \times 10^{-7}$ to $9 \times 10^{-5}$ Torr.

$Si_{Ga}$–$V_{Ga}$ complex by a species which is likely to be enhanced at high $SiH_4$ concentrations. The most likely candidate is $Si_{As}$, since the compensated character of the samples implies that also the $Si_{As}$ concentration increases as a function of $SiH_4$ partial pressure. The characteristics emission at 1.05 eV therefore may tentatively be attributed to the $Si_{Ga}$–$Si_{As}$ [42] complex. One can propose that Si atoms may be incorporated on both $Ga(Si_{Ga})$ and $As(Si_{As})$ lattice sites and that, the proportional Si atoms occupying the latter sites increases at higher total Si concentration. $Si_{As}$ centers are acceptors and so the expected free carrier concentration would be given by $n = [Si_{Ga}] - [Si_{As}]$. From this figure, it can also be seen that there is no peak at around 1.05–1.28 eV on those samples grown below $SiH_4$ partial pressure of $2.9 \times 10^{-5}$ Torr. Therefore, the peaks around 1.05–1.28 eV were present in those samples grown only at $SiH_4$ partial pressures greater than $2.9 \times 10^{-5}$ Torr and indicates that the film is compensated. It is a direct observation of autocompensation, by photoluminescence spectroscopy and confirmed by electrical methods and vice versa.

Fig. 5 was used for the determination of the full width at half maximum (FWHM) and the band gap narrowing (BGN). The FWHM, $\Delta E(n)$ of the B–B peak at 4.2 K of PL spectra increases with increasing electron concentration. The broadening of FWHM in Si-doped GaAs is similar to that in C-doped GaAs [53], Be doped GaAs [5] and Zn-doped GaAs [11,54] and can be explained by band to band optical transitions with and without momentum ($k$) conservation between the conduction and valence bands [11]. Alternatively, this can be explained in terms of the impurity band merging with the valence band edge and it becomes band tail states at high doping concentrations. Because of this phenomena, the optical transitions between the conduction and valence band are broadened and the FWHM of PL spectra increases. The $\Delta E(n)$ increases slowly up to $n \approx 2 \times 10^{17}$ cm$^{-3}$ and increases rapidly with increasing electron concentration. From the data we have obtained an empirical relation for FWHM of Si-doped GaAs,

$$\Delta E(n)(eV) = 1.4 \times 10^{-8} n^{1/3} \qquad (7)$$

with the concentration range between $1 \times 10^{17}$ and $1.5 \times 10^{18}$ cm$^{-3}$. The results are compared with previous studies reported in the literature [29] and shown in Fig. 6. The value of FWHM is about 5 meV for $n = 1 \times 10^{17}$ cm$^{-3}$, and it increases rapidly at $n > 3 \times 10^{17}$ cm$^{-3}$ due to the band filling.

### 3.2.2. PL spectra as a function of growth temperature

Fig. 7 shows the photoluminescence spectra at 4.2 K for all the samples studied in Fig. 2. From the Fig. 2, it is seen that the sample is autocompensated when the growth temperature is greater than 700°C in our
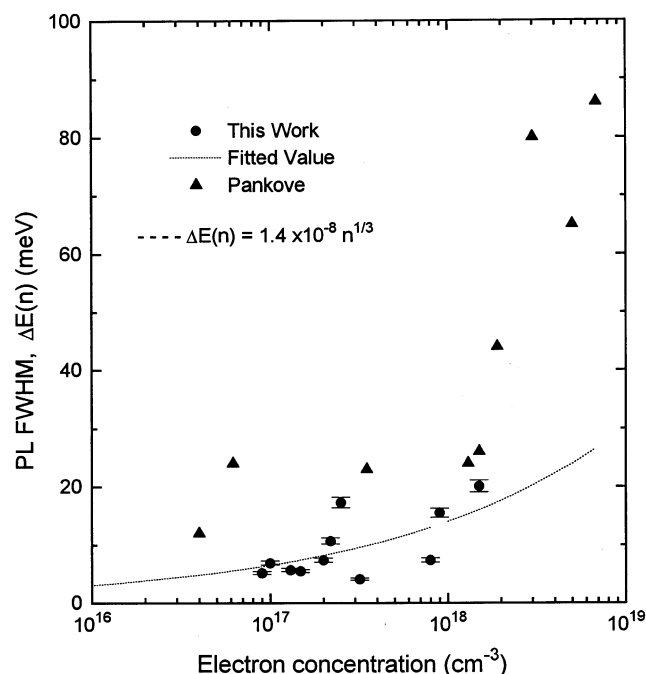


Fig. 6. FWHM of 4.2 K PL versus electron concentration.

present growth conditions. The PL spectrum corresponding to the growth temperature of 725°C is plotted as an inset in Fig. 7. The PL spectra shows a strong dependence on growth temperature. From this figure, it
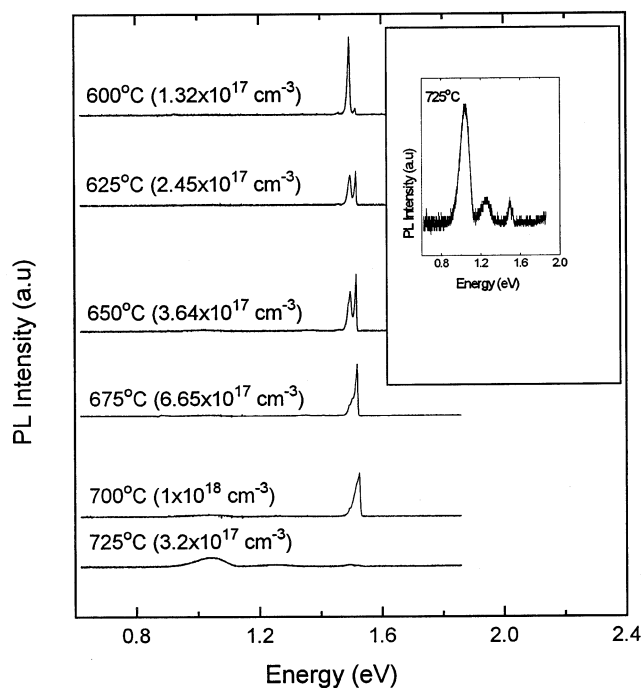


Fig. 7. A 4.2 K PL spectra of Si-doped GaAs epilayers for various growth temperatures. The growth parameters are: $[SiH_4] = 5.18 \times 10^{-7}$, $[TMGa] = 1.78 \times 10^{-4}$, $[AsH_3] = 1.57 \times 10^{-2}$. The inset shows the PL spectrum corresponds to the growth temperature at 725°C.

can also be seen that there is no peak around 1.05–1.28 eV on those samples grown below 700°C, whereas the peak around 1.05–1.28 eV was present in the sample grown at 725°C (inset in Fig. 7). This observation confirms that the film is autocompensated grown above 700°C, and exhibits consistently between the photoluminescence and electrical methods as well.

### 3.2.3. Band gap shrinkage due to doping effect

The excitonic PL main peak energy (1.5158 eV) shifted to higher energy as the electron concentration increased, which is primarily because of doping induced band gap shrinkage or band gap narrowing (BGN). From Fig. 5 it is seen that the peak position is nearly constant below $1.5 \times 10^{17}$ cm$^{-3}$, with a large increase in energy only for the most heavily doped sample, as the band filling effect becomes very significant. The doping dependence of peak energy position is in qualitative agreement with the literature [5,10,55]. However, the details of the B–B peak position plot, specifically the doping concentration where the band filling begins to drive the peak to higher energies, varies in the literature between $10^{18}$ and $10^{19}$ cm$^{-3}$. Also, one study [56] observed the peak position to decrease slightly with increasing doping for concentrations below $3 \times 10^{18}$ cm$^{-3}$, an effect which was attributed to BGN.

It is very difficult to extract the exact band gap shift from the PL spectra because of life time broadening effects [57]. We determined the band gap, $E_g$ of heavily doped GaAs, by a linear extrapolation to the energy axis, using a function of the type $f(E) = A(E - E_g)^{1/2}$, of the spectrum to the background level following the work by Olego and Cardona [11]. This method was used by several authors for determination of $E_g$. However, theoretical calculations [31,58,59] for $n$-GaAs indicate that BGN is strongly wave vector dependent for that material with the largest shifting occurring at zone center and much smaller shifts occurring near the Fermi energy. The BGN near the Brillouin zone center is extracted from the low-energy side of our PL spectral peaks and compared with a theoretical estimate of BGN at zone center. Fig. 8 shows the band gap shrinkage of Si-doped GaAs in the range $1 \times 10^{17}$–$1.5 \times 10^{18}$ cm$^{-3}$, as a function of electron concentration. In general, the band gap shrinkage is proportional to the electron concentration of the form $n^{1/3}$, thus it can be represented by

$$\Delta E_g = E_g(\text{doped}) - E_g(\text{pure}) = -Bn^{1/3} \tag{8}$$

where $B$ has been adjusted to give the measured value of $E_g$ at higher electron concentrations and the minus sign signifies the band gap shrinkage at higher concentrations. The empirical relation for band gap narrowing with our data can be written as
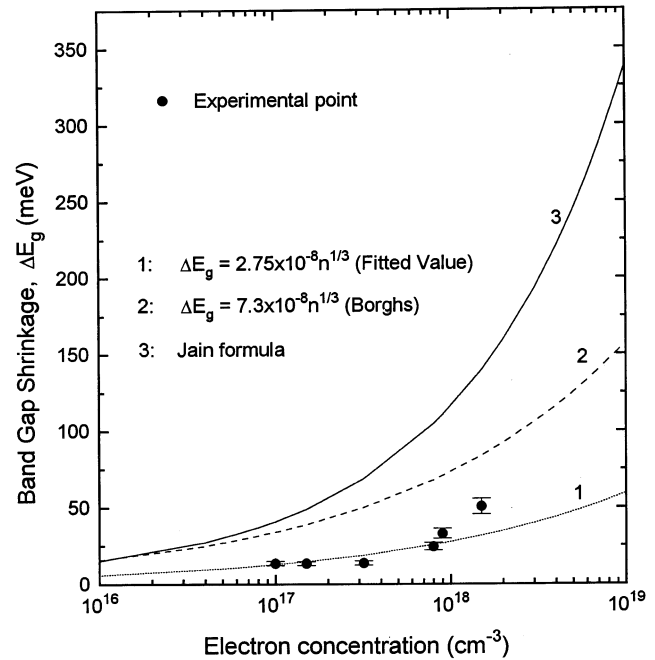
$$\Delta E_g = -2.75 \times 10^{-8} n^{1/3} \tag{9}$$



Fig. 8. The band gap shrinkage of Si-doped GaAs epilayers as function of electron concentration.

where $\Delta E_g$ is in eV and $n$ in cm$^{-3}$.

We have made an attempt to fit our experimental data to the expression suggested by Jain [60],

$$E_g = E_g(0) - \Delta E_g(n) \tag{10}$$

where $\Delta E_g(n) = a \times n^{1/3} + b \times n^{1/4} + c \times n^{1/2}$, $a$, $b$ and $c$ are the coefficients that represent the effects of the BGN due to majority–majority carrier exchange, minority–majority correlation and carrier-ion interaction, respectively. For $n$-type GaAs, the constants $a$, $b$ and $c$ are $16.5 \times 10^{-9}$, $2.39 \times 10^{-7}$ and $91.4 \times 10^{-12}$, respectively, where $n$ is the electron concentration in cm$^{-3}$ and $\Delta E_g(n)$ in eV. These relations are considered to provide a useful tool for determination of electron concentration in Si-doped GaAs by low temperature PL measurement. Good experimental agreement has been obtained for Eq. (10) in the cases of $p$-GaSb and $p$-GaAs [54,60]. Earlier work [61] on the group IV semiconductors Si and Ge using essentially the same formulation as Eq. (10) also showed good experimental agreement for $n$-Si $p$-Si and $n$-Ge. This good experimental agreement, coupled with the simplicity of the formula, makes Eq. (10) a valuable tool for semiconductor device modeling, assuming that the proper corrections are made to convert the physical BGN given by Eq. (10) to the apparent BGN used in device modeling [60,61]. In the case of $n$-GaAs, however, the agreement with experimental results is far from satisfactory [5,7], with Eq. (10) giving much larger BGN values than have been observed experimentally by PL. A similar discrepancy occurs even in $n$-InP [48].

To derive the experimental BGN, the extent of the low energy side of the B–B peak was defined as the point where the B–B peak merged with the noise level, which was about three orders of magnitude below the peak height for all low temperature (LT) sample spectra. Extrapolation of the low-energy side on a logarithmic plot was necessary for samples having electron concentrations $1 \times 10^{17}$, $1.5 \times 10^{17}$, $3.2 \times 10^{17}$ cm$^{-3}$ to avoid interference from the partially overlapping C–A peak. For samples having electron concentrations $8 \times 10^{17}$, $9 \times 10^{17}$ and $1.5 \times 10^{18}$ cm$^{-3}$, the C–A and B–B peaks were indistinguishable, and so the band tail extent of this single peak was taken. The BGN is thus defined as the difference between the intrinsic band gap $E_{go}$ and the band tail extent. The discrepancy of BGN between the experimental result and the Jain theory is clearly seen at high doping level. Very similar discrepancies have been observed for $n$-InP [48]. Sieg and Ringel [48] have given three possible explanations in the case of $n$-GaAs and $n$-InP between the theoretical BGN calculated from Eq. (10) and experimental BGN obtained by PL.

### 3.2.4. Effect of AsH₃ variation on PL spectra

To observe the effect of V/III ratio on the optical properties of Si-doped GaAs, the PL measurements were carried out at 4.2 K specifically on those samples grown at different AsH$_3$ flow rates. Fig. 9 shows the PL spectra of Si-doped GaAs for fixed TMGa and SiH$_4$ mole fraction. The three curves represent three different
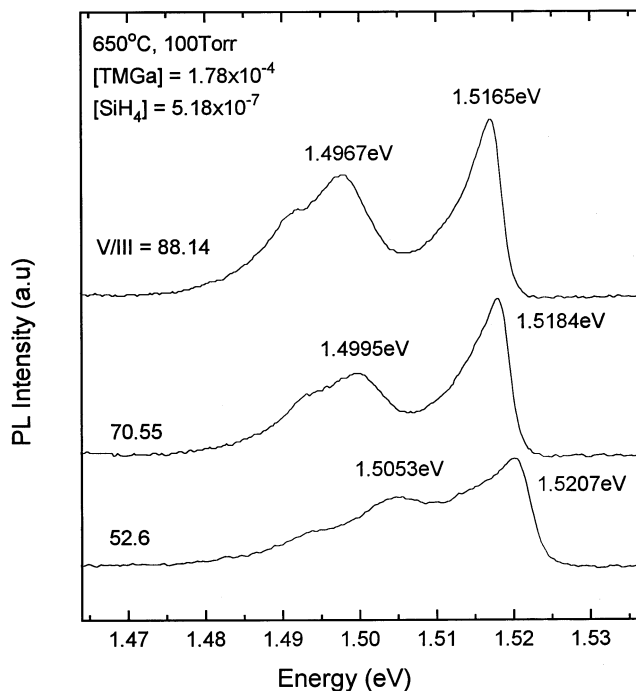


Fig. 9. A 4.2 K PL spectra of Si-doped GaAs epilayers as a function of AsH$_3$ flow rate.
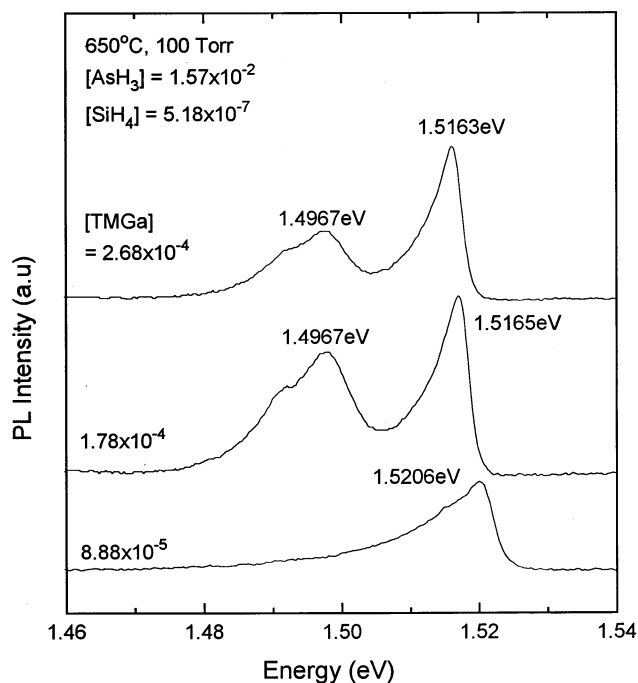


Fig. 10. A 4.2 K PL spectra of Si-doped GaAs epilayers as a function of TMGa flow rate.

AsH$_3$ flow rates. It is seen from the figure that the PL main peak energy shifts to lower photon energies since the electron concentration decreases with increasing AsH$_3$ mole fractions. The electron concentration decreases with the increasing V/III ratio for a given TMGa mole fraction and growth temperature of Si-doped GaAs, which is same as described by Bass [19]. At the V/III ratio of 52.6, the growth induced point defect at 1.5053 eV called Künzel–Ploog defect excitation was observed similar to that observed in MBE grown GaAs [62]. Even at this V/III ratio, the C–A or D–A transition is not observed whereas it is frequently found at MOVPE grown GaAs. These transitions may be absent in heavily doped materials. From these observations and from Hall mobility data, the highly doped layers were not caused by amphoteric nature of Si. On the other hand, the peak at 1.4967 and 1.4995 eV can influence the electrical properties of lightly doped layers. These peaks may be attributed to Zn and C (2S), respectively. The peak is asymmetric at lower AsH$_3$ mole fraction and becomes symmetric at higher AsH$_3$ mole fraction.

### 3.2.5. Effect of TMGa variation on PL spectra

To observe the effect of TMGa mole fraction on the optical properties of Si-doped GaAs, the PL measurement were carried out at 4.2 K specifically on those samples grown at different TMGa flow rates. Fig. 10 shows the PL spectra of Si-doped GaAs for fixed AsH$_3$ and SiH$_4$ mole fraction. The three curves represent three different TMGa flow rates. It is seen from the

figure that the PL main peak energy shifts to lower photon energies since the electron concentration decreases with increasing TMGa mole fractions. From Eq. (6) we found that a decrease in $P_{TMGa}$ will increase the Ga-vacancy concentration. Since Si incorporates in Ga site, the electron concentration increases with decreasing TMGa flow rates and hence the PL peak energy shifted to high photon energy. The PL data used in Figs. 9 and 10 are similar with our earlier paper [63], however these are included in the present paper in light of the discussion associated with other data presented.

## 4. Conclusions

Si-doped GaAs epitaxial layers grown by low pressure metalorganic vapor phase epitaxy in the electron concentration range $1 \times 10^{17}$–$1.5 \times 10^{18}$ cm$^{-3}$ have been investigated by photoluminescence as a function of electron concentration. Our results indicate the presence of Si complex defects, which are tentatively attributed to $Si_{Ga}$–$Si_{As}$. The $Si_{Ga}$–$Si_{As}$ pair defect is also present in heavily doped samples and also in the samples grown at higher growth temperatures. The photoluminescence spectra shows a strong dependence on electron concentrations and growth temperatures. We have demonstrated the direct correlation of autocompensation in both electrical and optical methods. From the PL spectra we have obtained an empirical relation of FWHM and band gap shrinkage as a function of electron concentrations. These relations are considered to provide a useful tool for determining the electron concentration by low temperature PL measurement. The B–B peak shifts to higher energy with increasing electron concentrations due to Burstein–Moss shift. Band-acceptor transitions involving residual C acceptors are the dominant recombination processes at concentration below $3.2 \times 10^{17}$ cm$^{-3}$. Above $3.2 \times 10^{17}$ cm$^{-3}$, however, the dominating contribution to the spontaneous recombination process in *n*-type GaAs arises from (indirect) transitions between free electrons in the conduction band and localized acceptor like centers in the deep tail states above the valence band edge. The B–B peak also shifts to high energy site as the AsH$_3$ and TMGa mole fraction decreases. The peak shift towards the lower energy side with increasing TMGa variation has been explained by vacancy controlled model.

## Acknowledgements

## References

[1] H.M. Manasevit, W.I. Simpson, J. Electrochem. Soc. 116 (1969) 1725.

[2] P.M. Solomon, Proc. IEEE 70 (1982) 489.

[3] H.C. Casey Jr., F. Stern, J. Appl. Phys. 47 (1976) 631.

[4] (a) E. Burstein, Phys. Rev. 93 (1954) 632. (b) T.S. Moss, Proc. Phys. Soc. London. B 67 (1954) 775.

[5] G. Borghs, K. Bhattacharyya, K. Deneffe, et al., J. Appl. Phys. 66 (1989) 4381.

[6] J. De-Sheng, Y. Makita, K. Ploog, et al., J. Appl. Phys. 53 (1982) 999.

[7] H. Yao, A. Compaan, Appl. Phys. Lett. 57 (1990) 147.

[8] R. Visser, H.G.M. Lochs, L.J. Gilling, J. Appl. Phys. 68 (1990) 5819.

[9] C. Lee, N.Y. Lee, K.J. Lee, et al., J. Appl. Phys. 77 (1995) 6727.

[10] N.Y. Lee, K.J. Lee, C. Lee, et al., J. Appl. Phys. 78 (1995) 3367.

[11] D. Olego, M. Cardona, Phys. Rev. B 22 (1980) 886.

[12] A. Silberman, T.J. Delyon, J.M. Woodall, Appl. Phys. Lett. 58 (1991) 2126.

[13] B.G. Arnaudor, V.A. Vilkotskii, D.S. Domanerskii, et al., Sov. Phys. Semicond. 11 (1977) 1054.

[14] A. Bignazzi, A. Bosacchi, R. Magnanini, J. Appl. Phys. 81 (1997) 7540.

[15] J.M. Redwing, Ph.D Thesis, University of Wisconsin-Madison, 1994.

[16] R.J. Field, S.K. Ghandhi, J. Cryst. Growth 74 (1986) 543.

[17] R.J. Field, S.K. Ghandhi, J. Cryst. Growth 74 (1986) 551.

[18] S.J. Bass, P.E. Oliver, Inst. Phys. Conf. Ser. (Inst. Phys. Lond.) 33b (1977) 1.

[19] S.J. Bass, J. Cryst. Growth 47 (1979) 613.

[20] M.K Lee, C.Y. Chang, Y.K Su, Appl. Phys. Lett. 42 (1983) 88.

[21] R. Azoulay, L. Dugrand, D. Ankri, et al., J. Cryst. Growth 68 (1984) 453.

[22] S.Z. Sun, E.A. Armour, K. Zheng, et al., J. Cryst. Growth 113 (1991) 103.

[23] D. Shaw, Atomic Diffusion in Semiconductors, Plenum, New York, 1973.

[24] M.E. Greiner, J.F. Gibbons, Appl. Phys. Lett. 44 (1984) 750.

[25] W. Walukiewicz, Appl. Phys. Lett. 54 (1989) 2094.

[26] W. Walukiewicz, Phys. Rev. B 41 (1990) 10218.

[27] L.W. Yang, P.D. Wright, V. Eu, et al., J. Appl. Phys. 72 (1992) 2063.

[28] S.I. Kim, M.S. Kim, Y. Kim, et al., J. Appl. Phys. 73 (1993) 4703.

[29] J.I. Pankove, J. Appl. Phys. 39 (1968) 5368.

[30] D.A. Cusano, Appl. Phys. Lett. 7 (1965) 151.

[31] B.E. Sernelius, Phys. Rev. B 33 (1986) 8582.

[32] E.F. Schubert, Doping in III–V Semiconductors, Cambridge University, Cambridge, 1993.

[33] H. Fushimi, M. Shinohara, K. Wada, J. Appl. Phys. 81 (1997) 1745.

[34] T.N. Theis, P.M. Mooney, S.L. Wright, Phys. Rev. Lett. 60 (1988) 361.

[35] V. Swaminathan, M.D. Sturge, J.L. Zilko, J. Appl. Phys. 52 (1981) 6306.

[36] E.F. Schubert, E.O. Göbel, Y. Horikoshi, et al., Phys. Rev. B 30 (1984) 813.

[37] T. Oh-hory, H. Itoh, H. Tanaka, et al., J. Appl. Phys. 61 (1987) 4603.

[38] S. Adachi, J. Appl. Phys. 63 (1988) 64.

[39] A.M. De Paula, G. Medeiros-Ribeiro, A.G. De Oliveira, J. Appl. Phys. 76 (1994) 8051.

[40] R. Venkatasubramanian, K. Patel, S.K. Ghandhi, J. Cryst. Growth 94 (1989) 34.

[41] P.L. Souza, E.V.K. Rao, J. Appl. Phys. 67 (1990) 7013.

[42] E.P. Visser, X. Tang, R.W. Wieleman, et al., J. Appl. Phys. 69 (1991) 3266.

[43] J. Maguire, R. Murray, R.C. Newman, et al., Appl. Phys. Lett. 50 (1987) 516.

[44] E. Veuhoff, T.F. Kuech, B.S. Meyerson, J. Electrochem. Soc. 132 (1985) 1958.

[45] J.P. Duchemin, M. Bonnet, F. Koelsch, et al., J. Electrochem. Soc. 126 (1979) 1134.

[46] V. Swaminathan, D.L. Van Haren, J.L. Zilko, et al., J. Appl. Phys. 57 (1985) 5349.

[47] D.J. Ashen, P.J. Dean, D.T.J. Hurle, et al., J. Phys. Chem. Solids 36 (1975) 1041.

[48] R.M. Sieg, S.A. Ringel, J. Appl. Phys. 80 (1996) 446.

[49] V.A. Vilkotskii, D.S. Dornamevskii, R.D. Kakanov, et al., Phys. Status Solidi B 91 (1979) 71.

[50] A.P. Levanyuk, V.V. Osipov, Sov. Phys. Semicond. 7 (1973) 721.

[51] E.W. Williams, H.B. Bebb, in: R.K. Willardson, A.C. Beer (Eds.), Semiconductors and Semimetals, vol. 8, Academic, New York, 1972 chp. 5.

[52] X. Tang, H.G.M. Lochs, P.R Hageman, et al., J. Cryst. Growth 98 (1989) 827.

[53] S.I. Kim, M.S. Kim, S.K. Kim, et al., J. Appl. Phys. 74 (1993) 6128.

[54] M.K. Hudait, P. Modak, S. Hardikar, et al., J. Appl. Phys. 82 (1997) 4931.

[55] M. Druminski, H.D. Wolf, K.H. Zschauer, et al., J. Cryst. Growth 57 (1982) 318.

[56] M. Bugajski, W. Lewandowski, J. Appl. Phys. 57 (1985) 521.

[57] B.E. Sernelius, Phys. Rev. B 34 (1986) 5610.

[58] J.R. Lowney, J. Appl. Phys. 60 (1986) 2854.

[59] H.S. Bennett, J.R. Lowney, J. Appl. Phys. 62 (1987) 521.

[60] S.C. Jain, J.M. McGregor, D.J. Roulston, J. Appl. Phys. 68 (1990) 3747.

[61] S.C. Jain, D.J. Roulston, Solid-State Electron. 34 (1991) 453.

[62] H. Künzel, K. Ploog, Appl. Phys. Lett. 37 (1980) 416.

[63] M.K. Hudait, P. Modak, S. Hardikar, et al., Math. Sci. Eng. B 55 (1998) 53.